Chapter 16 – MODEL VALIDATION: FUSELAGE LAP JOINTS

Graeme F. Eastaugh and Ali Merati
Institute for Aerospace Research
National Research Council Canada
Ottawa, Ontario
CANADA

Paul V. Straznicky
Department of Mechanical and Aerospace Engineering, Carleton University
Ottawa, Ontario
CANADA

16.1 INTRODUCTION

While current design and maintenance guidelines and procurement specifications provide a good structural integrity framework for new aircraft and the reassessment of existing aircraft, there remains a risk that Corrosion Fatigue Interaction (CFI) can undermine the margins of safety in the durability or damage tolerance assessments as they are currently performed. This statement applies to all forms of corrosion, including pitting, stress corrosion cracking, crevice, galvanic, filiform, and exfoliation corrosion. It also applies to all forms of CFI, some of which may be dependent on the geometry and other features of the structural component in question. This risk is unquantified, because most manufacturers and operators treat corrosion and fatigue as separate issues during design, and they assume that the design and the maintenance program will obviate any serious interaction.

There might be several reasons why some people believe that corrosion fatigue interaction need not or cannot be taken into account. They are summed up as follows:

a) In damage tolerant structure, fatigue cracks will be detected before they reach critical size, and so the cause of the fatigue cracks does not significantly influence the risk of structural failure.

b) In safe life structure, the large safety margins (scatter factors) applied to the estimated fatigue life take into account unknowns such as corrosion.

c) While corrosion is widespread on aircraft, no fatigue cracks are found at corrosion sites and no catastrophic failures have recently been attributed to corrosion. Hence corrosion is thought to be an economic problem but not a safety problem.

d) There are no widely accepted models for predicting the onset and the effects of corrosion fatigue interaction and thereby estimating the associated risk.

The first three reasons are not considered to be valid. With regard to a), if corrosion fatigue interaction is not considered in damage tolerance analysis some potential failure modes of Structurally Significant Items (SSI) will be overlooked, and some components that should be regarded as SSI will not be analyzed. Consequently, insufficient components will be included in the targeted inspection program and some of those that are included will not be inspected in an appropriate manner.

With regard to b), the safety factors of between three and five currently in use for safe life structure derive primarily from the variability noted in accelerated fatigue tests in ambient air and the need to work with small sample sizes. They do not make a specific allowance for life reduction due to CFI under operating conditions. Much larger factors would be needed for this purpose, as proposed by Schütz [1].

With regard to c), the high annual cost of corrosion related maintenance – estimated to be over $1B in the USAF [2] – is a testament to the underlying danger of premature structural failure due to corrosion fatigue interaction. Therefore, it is difficult to see how a general argument can be made that corrosion only presents an economic problem. Fortunately, catastrophic structural failures in aircraft are rare, and so catastrophic failures due to corrosion fatigue interaction are also rare. But they do occur. Furthermore, a thorough investigation (failure analysis) is needed to fully understand the degradation mechanisms. In most cases of corrosion, this is not necessary or cost-effective. Therefore, it is not possible to generalize that corrosion found in service on highly stressed components is not already interacting with fatigue.

The last reason, d), is valid. It is the justification for the considerable effort expended in the USA and Canada over many years to investigate ways of modeling corrosion fatigue interaction in aircraft structure. This effort has been driven by the high cost of corrosion related maintenance in terms of resources and aircraft down-time. Modeling of corrosion fatigue interaction is expected to help reduce maintenance costs and improve aircraft availability. If successful, it will provide the means to design structure with tolerance to this form of degradation, and it will allow alternative responses to a corrosion occurrence in service to be evaluated. The ways in which assessments of corrosion fatigue interaction can be included in the Aircraft Structural Integrity Programs (ASIP) followed by the USAF and other air forces were outlined in a landmark paper by Brooks and Simpson [3].

Unfortunately, the modeling of corrosion fatigue interaction is a difficult topic, even for simple components. It is important to study and model the fundamental mechanisms of such interaction, but it is also important to use traditional engineering methods to understand and model it at the component level. This section presents a study of the effects of corrosion on the fatigue characteristics of a riveted fuselage skin splice. This is a complex component with complex failure mechanisms, including a failure mode known as Multiple Site Damage (MSD). One of the aims of the study was to determine whether it might be feasible despite this complexity to construct a useful empirical model of the effects of prior corrosion on fatigue life and crack growth characteristics. If successful, the approach could be cost-effective to apply, since fuselage skin splices are one of the most widespread and corrosion-prone structural details on transport aircraft. The aim was achieved by manufacturing and fatigue testing a specially designed splice specimen under controlled conditions to produce statistically significant results. Fifty percent of the test specimens were pre-corroded. The test program is outlined, and a probabilistic model based on the test results is proposed that could be used in durability, damage tolerance, and risk analyses.

16.2 EXPERIMENTAL PROCEDURES

16.2.1 Description of Lap Splice Specimen

The splice element is a single shear lap splice 8.0 in. (203.2 mm) long with 3 rows of 5/32 in. (4.0 mm) diameter rivets at 1 in. (25.4 mm) pitch in the hoop and longitudinal directions. The spliced sheets are 0.040 in. (1.0 mm) thick 2024-T3 aluminum alloy clad both sides without any other surface treatments. Single shear lap splices of this approximate configuration are used in the fuselages of the KC-135, JSTARS, C-130, and P-3 aircraft. However, in this study, the results are intended for the development of a general modelling approach and should not be applied directly to any specific aircraft. For specific studies, the design of the specimen should be tailored to the aircraft splice in question, taking care to simulate correctly the out-of-plane bending stresses and the load transfer from cracked regions.

The specimen complete with the clamping plates and pins used to mount it in the load frame is shown in the drawing and photograph in Figure 16-1. In this figure, the specimen is shown with the splice oriented as though being viewed from outside an aircraft. The upper sheet in this view is the countersunk sheet. The lower sheet is referred to as the driven sheet. The specimen was designed to simulate the stress conditions and MSD failure mode experienced by fuselage skin splices. Back-to- back strain gauges were placed in rows 1 in. (25.4 mm) above and below the splice to record the nominal stress distribution across the

specimen. Additional detail on the specimen and the general procedure for adapting the MSD specimen concept to a specific aircraft splice are in [4].

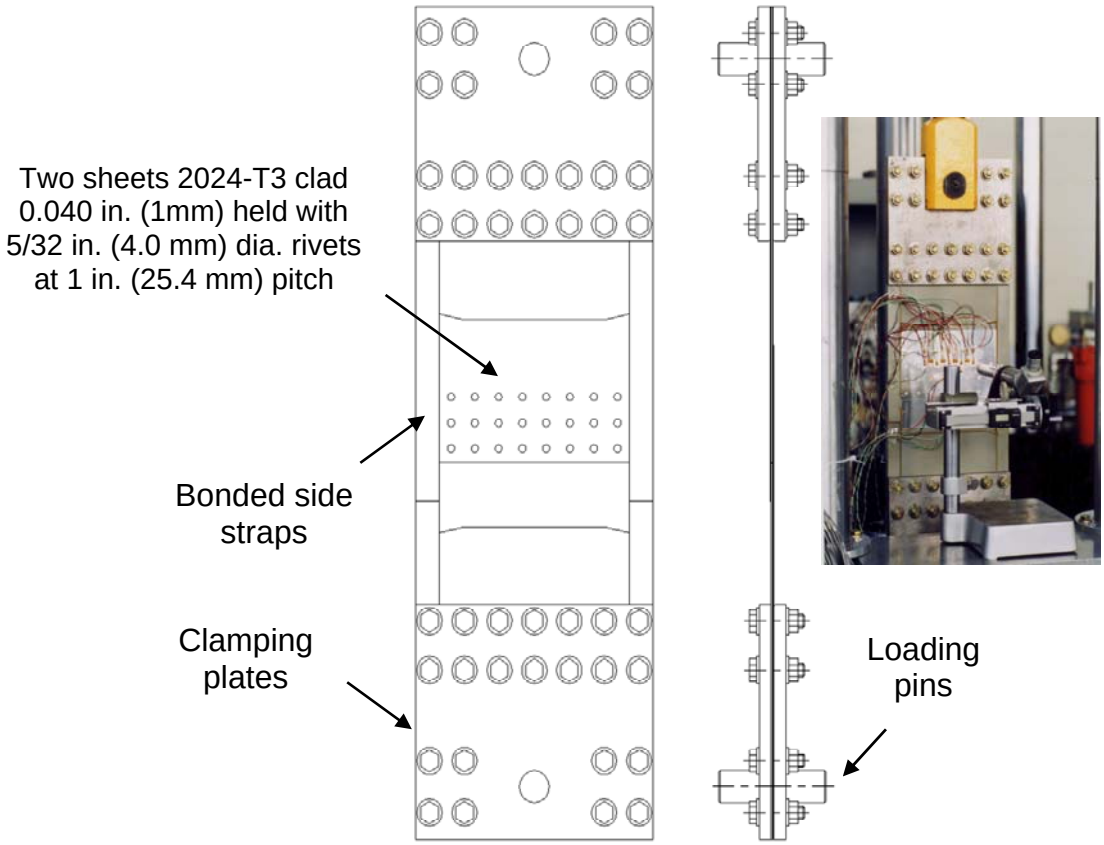

Figure 16-1: Lap Splice Specimen with Clamping Plates and Loading Pins (the left-hand drawing shows the splice as it would appear from outside an aircraft).

16.2.2 Preparation of Corroded Specimens

The specimens to be corroded were selected randomly. The interior of the splice was corroded and dried prior to fatigue testing. The target range of corrosion severity had been observed in several lap splices from service aircraft. It was a moderate level that might go unnoticed during routine visual inspection for corrosion pillowing. The corrosion procedure was developed during a pilot test program. It was not expected to simulate accurately the iterative, mainly sequential process of corrosion and fatigue that occurs on aircraft over many years in service. However, it was expected to provide evidence of some of the mechanisms of interaction of corrosion and fatigue in service and to provide a statistically significant indication of the effect of typical corrosion on fatigue characteristics. More information on the corrosion procedure and its simulation of service corrosion can be found in [5].

The corrosion build-up inside the splice caused pillowing distortion. This distortion can be seen clearly in comparing the images of corroded and non-corroded specimens in Figure 16-2, which were obtained using the D Sight Aircraft Inspection System (DAIS). The distortion can significantly affect the stress distribution in a splice, and has been modeled in other work at the National Research Council (NRC) Canada [6]. Measurements of pillowing distortion were used to monitor the level of corrosion during the pre-corrosion process.

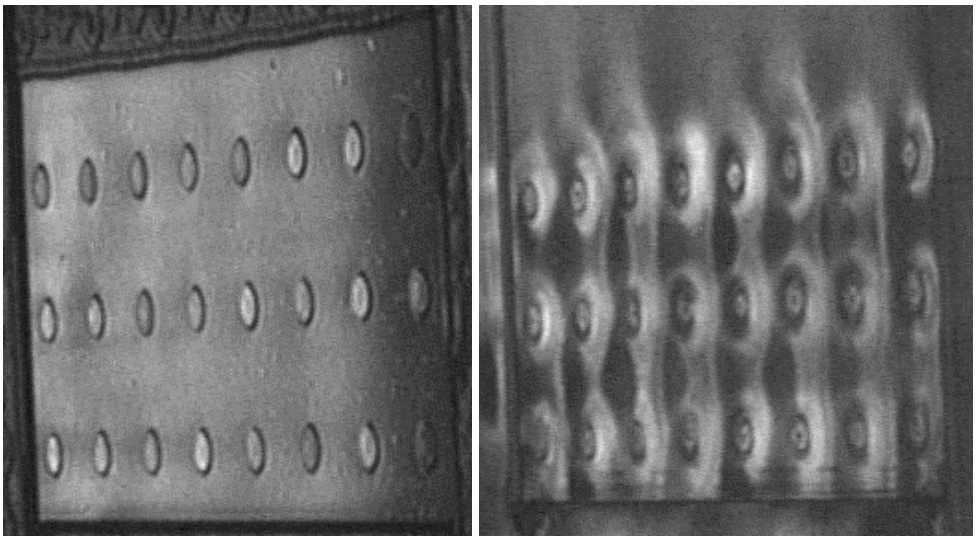

Figure 16-2: D Sight Aircraft Inspection System (DAIS) Images of a Lap Splice Specimen Before Corrosion (left) and After Corrosion (right).

16.2.3 Fatigue Testing

Nine non-corroded and nine corroded specimens were fatigue tested. The approach followed ASTM guidelines for a paired comparison test program [7] as far as practicable. Various other precautions were taken to minimize nuisance variables that might mask the effects of corrosion on fatigue characteristics.

All specimens were subjected to constant amplitude, uniaxial, cyclic loading at 4 Hz using a MTS servo hydraulic load frame. The fatigue test was load controlled, with a load ratio of 0.02. After cracks emerged from under the rivet heads they were measured using a travelling microscope. The tests were generally allowed to continue until cracks had developed and linked up across the full width of the splice. The specimen did not break apart at this point, because the side straps carried the maximum load. A few tests were terminated earlier for various reasons.

16.2.4 Measurement of Corrosion Damage

In the case of fuselage splices, it is currently difficult to measure the hidden corrosion damage at the faying surfaces, i.e., the internal contacting surfaces, accurately and with high resolution using Non-Destructive Inspection (NDI). Therefore, the corrosion damage was measured throughout each sheet after dismantling the splices. An efficient method of doing this over large areas was developed by the NRC several years ago, and procedures have been progressively improved. It involves dismantling the splice and removing the corrosion products chemically from each sheet (Figure 16-3). Then each sheet is radiographed using X-rays. Various calibration pieces of known thickness are included in the radiograph. The radiograph is digitized, calibrated, and analyzed using custom and commercial image processing software. Measurements of the average thickness loss in specific areas of interest were obtained from the grey scale versions of the radiographs. The grey scale radiographs were also colorized to provide calibrated thickness maps for general study and comparison with NDI (Figure 16-4). The X-ray images are presented in standard orientation for this work, i.e., as though being viewed from the exterior of an aircraft. Thus, if the images for the countersunk and driven sheets were overlaid, they would indicate the total distribution of corrosion damage at the faying surfaces of the splice.

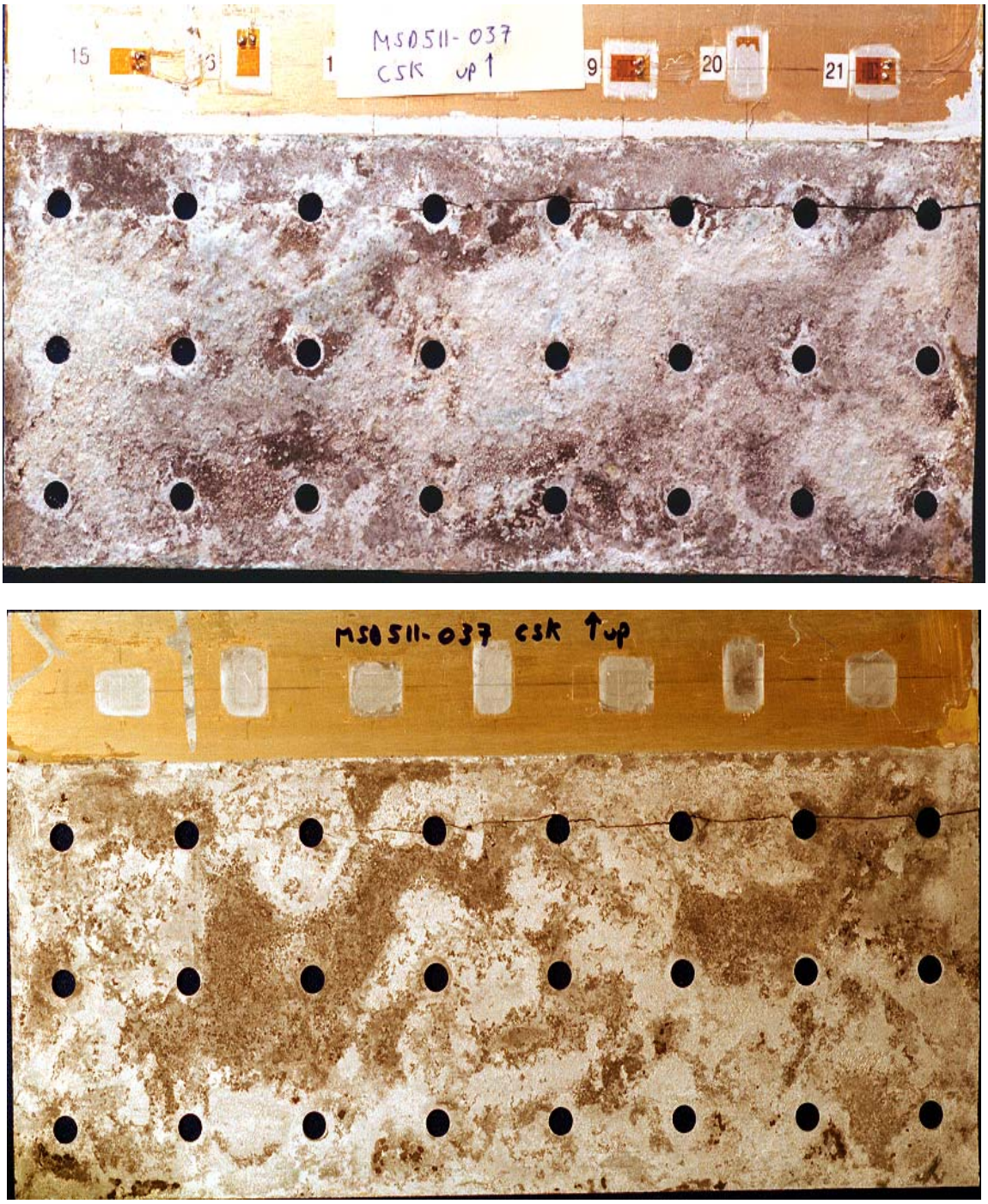

Figure 16-3: Faying Surface of the Countersunk Sheet of Specimen #037 Before and After the Removal of Corrosion Products.

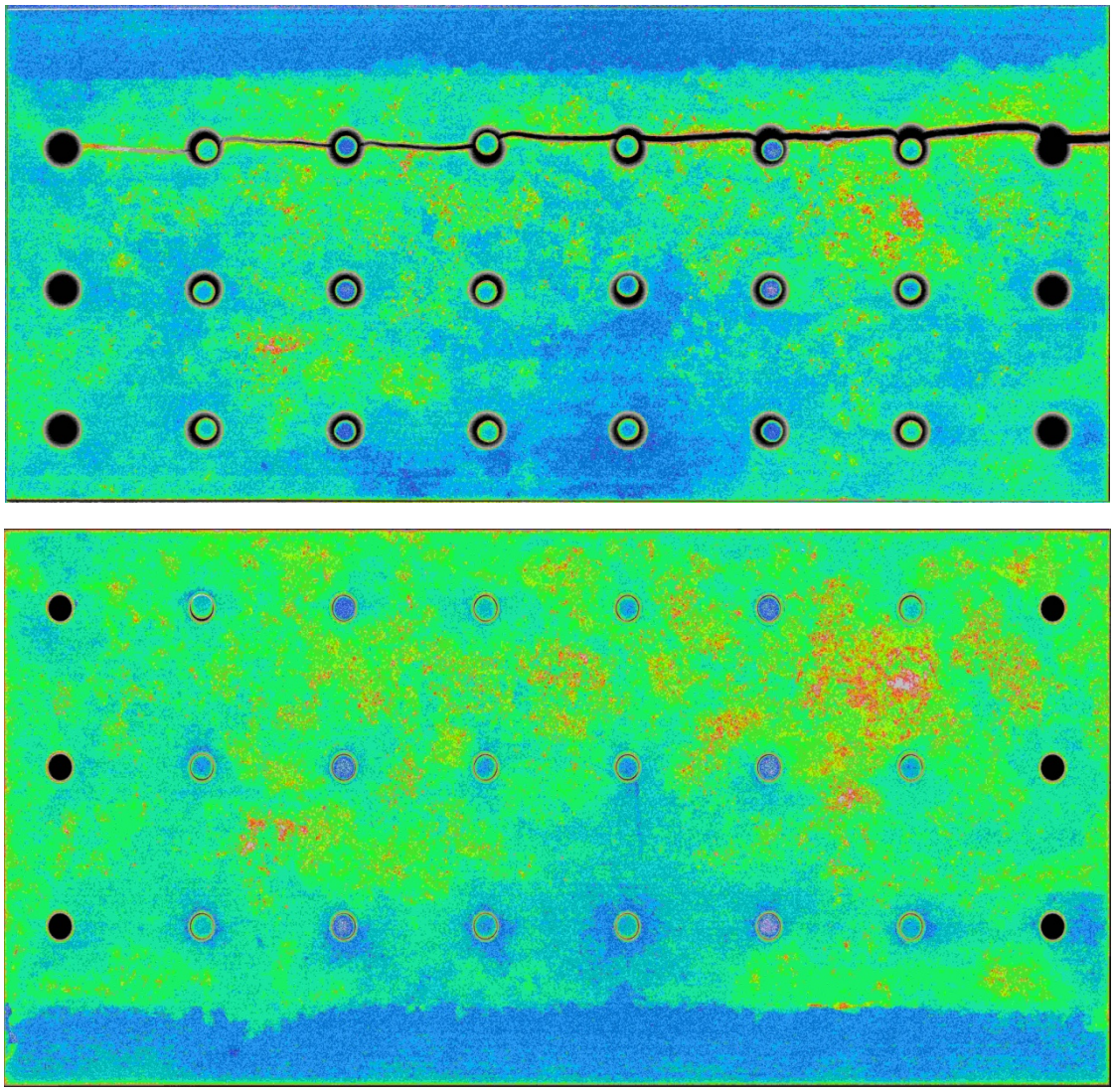

Thickness range (in.)		Thickness loss range (in.)		Thickness loss range (%)		Pseudo-color
Min	Max	Min	Max	Min	Max	
0.041						Light Grey
0.04	0.041		0		0.00%	Dark Blue
0.039	0.04	0	0.001	0.00%	2.50%	Light Blue
0.038	0.039	0.001	0.002	2.50%	5.00%	Green-Blue
0.037	0.038	0.002	0.003	5.00%	7.50%	Green
0.036	0.037	0.003	0.004	7.50%	10.00%	Orange
0.035	0.036	0.004	0.005	10.00%	12.50%	Red
	0.035	0.005		12.50%		Mid-Grey

Figure 16-4: Pseudo-Colored Digitized X-Ray (DXR) Thickness Maps Showing Corrosion Distribution in Countersunk (upper image) and Driven (lower image) Sheets of Specimen #035 (higher resolution grey scale images are used for quantitative analysis).

The measurements obtained from radiographs indicated that the overall average thickness loss varied between specimens. The average thickness loss per sheet in the corroded specimens was estimated to be in

the range of 3% to 6%. The term “average thickness loss per sheet” is used to signify that the data is a combined average of both sheets in a given location, expressed as a percentage of the original thickness of one sheet. As can be seen from the example of an X-ray thickness map, the depth of the corrosion damage in some locations within a splice was much higher than this average value.

16.3 RESULTS AND DISCUSSION

16.3.1 Failure Modes

All non-corroded specimens failed by cracking in the countersunk sheet along the upper rivet row. The set of individual crack growth curves on the left in Figure 16-5 illustrates the typical MSD failure mode of the non-corroded specimens.

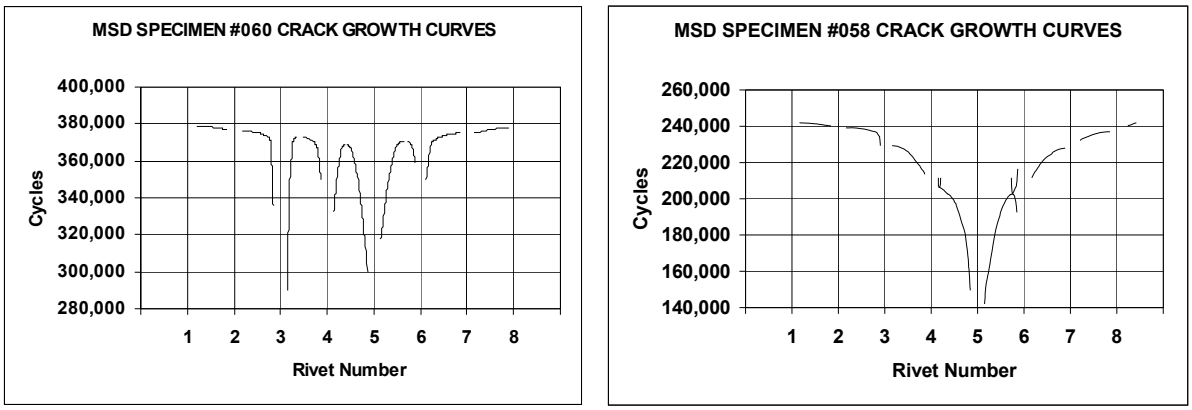

Figure 16-5: Example Sets of Individual Crack Growth Curves for Non-Corroded (left) and Corroded (right) Specimens.

Two general modes of failure were observed in the corroded specimens. Firstly, six out of nine specimens failed by cracking in the countersunk sheet along the upper rivet row. In these cases, the crack pattern was dominated by the early nucleation of cracks at one location. Thus a MSD pattern like the one in the non-corroded specimens did not develop. The right hand graph in Figure 16-5 illustrates this mode of failure. Secondly, three out of nine corroded specimens failed by cracking in the driven sheet, just below or along the lower rivet row. This mode of failure would be difficult to detect on an aircraft. Again, the crack pattern was dominated by the lead crack in each case. There were other, less obvious differences in the failure modes of the corroded and non-corroded specimens, but a discussion of these is outside the scope of this paper.

16.3.2 Empirical Modelling of the Effects of Corrosion on MSD Crack Growth and Fatigue Life

For the purpose of modeling the experimental data, the fatigue life of a specimen was divided into two parts: the life to the detection of the first crack, and the subsequent life to failure of the specimen. While MSD occurred in many cases, it was observed that the cracks invariably linked up progressively to form a single crack across the splice. A similar phenomenon has been observed in longitudinal fuselage skin splices on aircraft. Therefore, it was decided to investigate the possibility of characterizing the detectable crack growth in a splice by a single aggregate crack growth curve. Since the specimens were designed not to collapse when fully cracked, an aggregate crack length of 6 in. (152.4 mm) was defined as failure. If the test was terminated earlier, as was the case with some corroded specimens, the final crack length was used

without adjustment. Since the actual length of the first crack at detection varied between tests, the criterion for first detection for analytical purposes was defined as an aggregate crack length of 0.5 in. (12.7 mm). This criterion encompassed the actual detection of the first crack in all specimens except one, and is consistent with the smallest crack in a splice that can reliably be detected in service using eddy current inspection.

To provide an overview of the fatigue test results, the aggregate crack growth curves for detectable crack growth are presented first. These are in Figure 16-6. The curves were constructed by summing the lengths of all detected cracks in the manner indicated in the sketch. Each curve starts at the length at which the crack was actually detected during the fatigue test. The single point is for a test that was terminated as soon as the first crack was detected. The aggregate crack growth curves for corroded and non-corroded specimens are fairly closely grouped, except for the curves for two corroded specimens. As yet, no reason has been found for treating these two specimens as statistical outliers, and so they have been included in all the statistics for Corroded Sample A. This sample excludes only the specimen with the single point plot. For interest, some graphs in this paper include comparative statistics for a Corroded Sample B that excludes the specimen with the longest life.

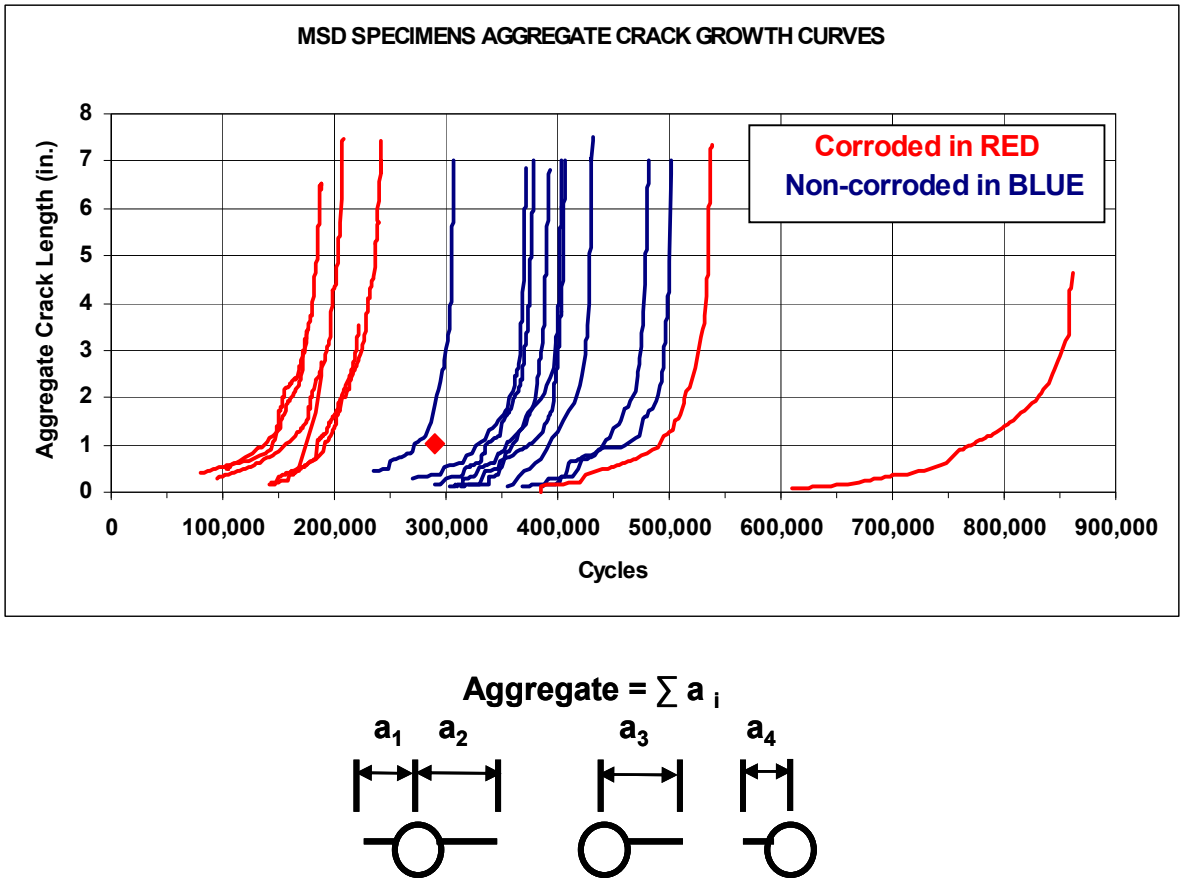

Figure 16-6: Aggregate Crack Growth Curves for Corroded and Non-Corroded Specimens.

The mean life to an aggregate crack length of 0.5 in. (12.7 mm) – i.e., to the first crack – is presented in Figure 16-7. In practice, an aggregate crack length of 0.5 in. (12.7 mm) implied two-sided cracking at one rivet, as illustrated in the sketch in the figure. The central bars represent the mean lives, while the accompanying pairs of bars represent the lower and upper bounds of the 90% confidence interval. The graph shows that pre-corrosion caused a statistically significant reduction in the life to the first crack.

The difference in mean lives indicates a 44% reduction in this portion of the life of the splice. The statistics for Corroded Sample B indicate a 54% reduction.

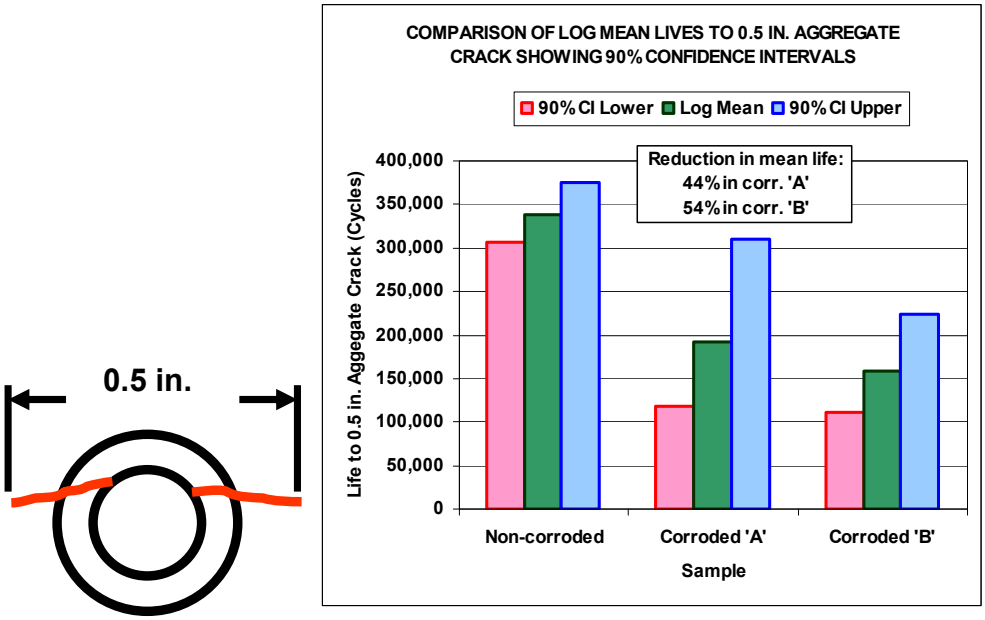

Figure 16-7: Mean Life to 0.5 in. Aggregate Crack with 90% Confidence Intervals.

The distribution of life to the first crack is presented in Figure 16-8. The graph shows the experimental data points plotted using a non-parametric distribution formula – i.e., one that does not require any prior assumption concerning the shape of the distribution. The graph superimposes the continuous curves obtained by fitting a Log Normal distribution to the data. These Log Normal curves are the probabilistic models of the life to the detection of the first crack for non-corroded and corroded specimens. The probability that the life to the first crack, N_1, has a certain value can be represented mathematically as follows:

$$P(N_1 [x) = F_{N1}(x) \quad (1)$$

where $F_{N1}(x)$ is a Log Normal cumulative distribution function whose mean and standard deviation are estimated from the test data. $F_{N1}(x)$ is different for corroded and non-corroded splices.

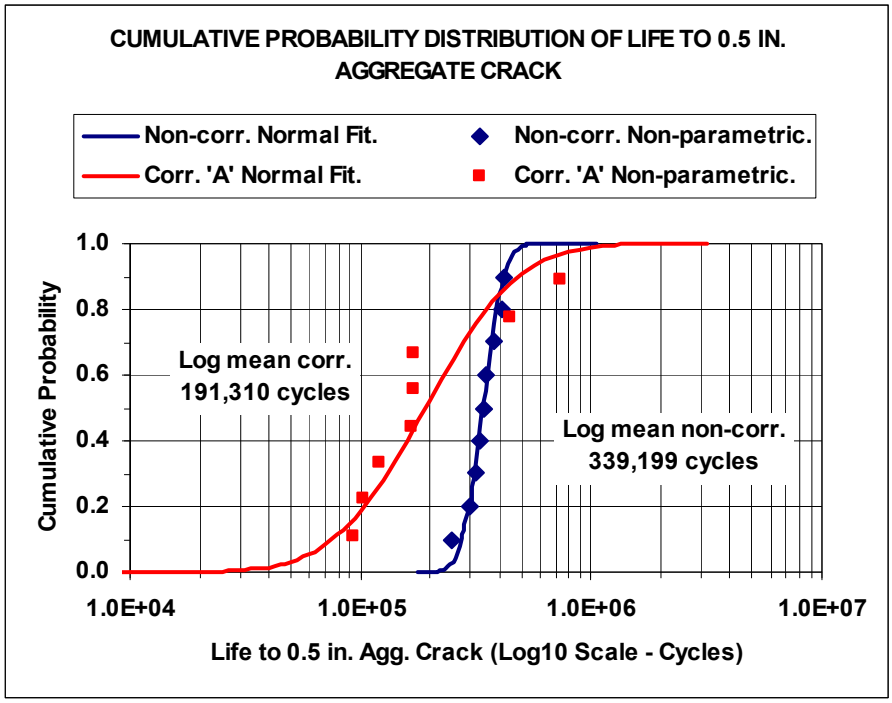

Figure 16-8: Empirical Models of Life to an Aggregate Crack Length of 0.5 in. (12.7 mm).

To model the subsequent period of detectable crack growth, the relationship between the aggregate crack growth rate per cycle, da/dN, and the aggregate crack length, a, was investigated and is presented in Figure 16-9. The left hand graph shows the relationship for a non-corroded specimen. The right hand graph shows the relationship for a corroded specimen. Similar analyses were performed for every specimen. Linear regression of the data for each specimen indicated that a relationship could be assumed of the form:

$$da/dN = Q.a^{m} \tag{2}$$

where m and Q are stochastic variables. This second phase model of multiple crack growth is comparable to the one proposed in [8] for a single crack in non-corroded structure. However, the analytical approach developed below is closer to the one used in [9] for the Paris-Erdogan equation.

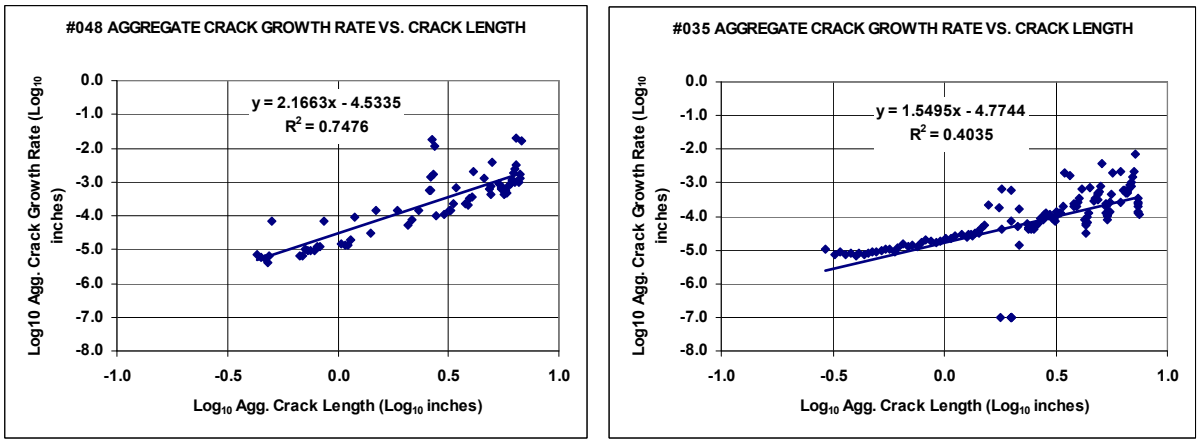

Figure 16-9: Illustration of the Relationship Between Aggregate Crack Growth Rate and Aggregate Crack Length in Non-Corroded (left) and Corroded Specimens (right).

From data of the kind illustrated in Figure 16-9, distributions for the exponent "m" were estimated for the corroded and non-corroded populations. The graph in Figure 16-10 shows the data points of the non-parametric analyses. The superimposed continuous curves are Normal distributions estimated from the experimental data. The Normal fits show reasonable agreement with the non-parametric analyses for both the corroded and the non-corroded populations. Similar distributions were developed for the parameter Q and are shown in Figure 16-11. Log Normal fits were assumed in this case. Based on these assumed curve fits, the probability that the parameters m and Q in Equation (2) have certain values can be represented by the following general equations:

$$P(m\ [\ x) = F_m(x) \tag{3}$$

$$P(Q\ [\ x) = F_Q(x) \tag{4}$$

where $F_m(x)$ is a Normal cumulative distribution function and $F_Q(x)$ is a Log Normal cumulative distribution function. The means and standard deviations of $F_m(x)$ and $F_Q(x)$ are estimated from test data. The functions will be different for non-corroded and corroded specimens.

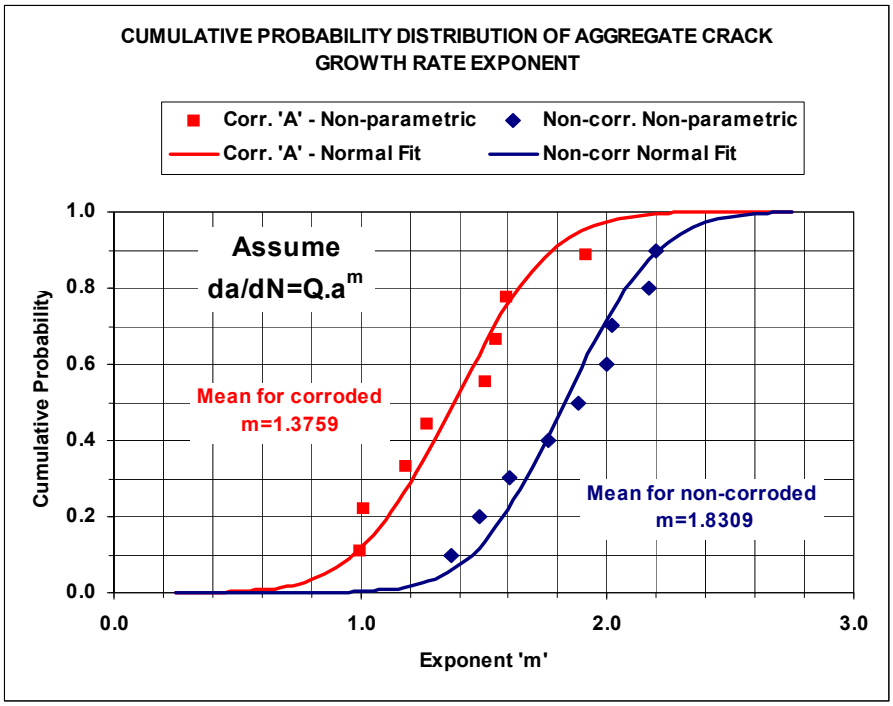

Figure 16-10: Distribution of Exponent 'm' in Equation da/dN = Q.a^m.

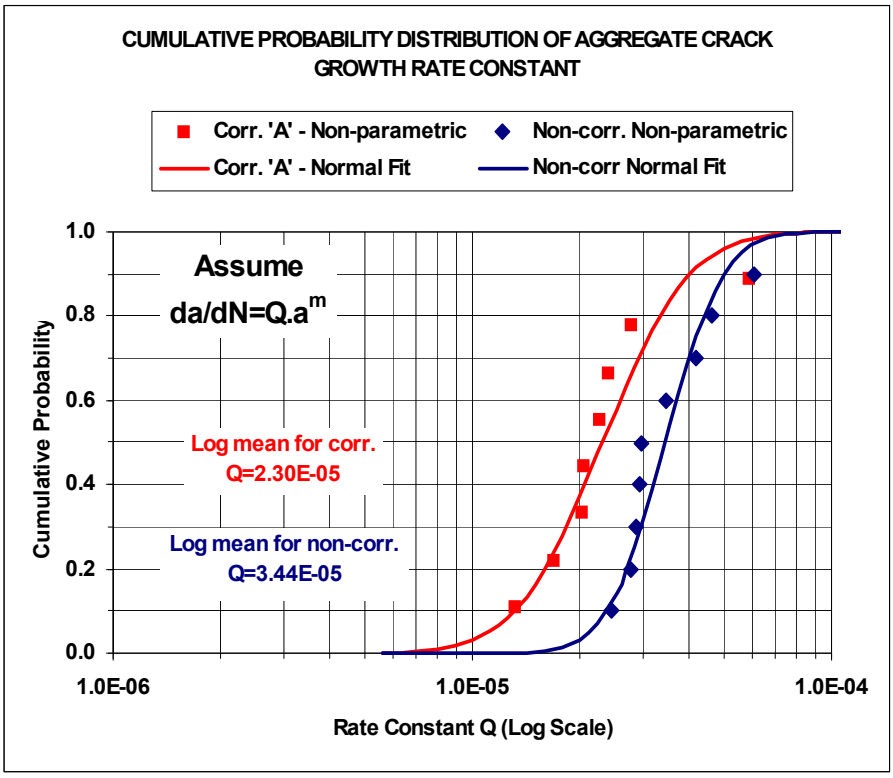

Figure 16-11: Distribution of Constant 'Q' in Equation da/dN = Q.a^m.

Equations (1) to (4) together represent a generalized probabilistic model of the whole fatigue life of a splice. The cumulative distribution functions of aggregate crack length at given values of the total life, $F_{a,\ Ntotal}(x)$, could be estimated from this model using a Monte Carlo simulation. This would involve repeated numerical integration of Equation (2) to generate a large sample of aggregate crack growth curves. For each simulation of a splice fatigue life, the parameters N_1, m, and Q, would be sampled according to their respective distributions using a random number method. Assuming constant amplitude loading, the probability of failure of the splice after a certain number of fatigue cycles, N_{total}, would be the probability that the crack length had exceeded the failure criterion:

$$P(a > 6 \text{ in.}) = 1 - F_{a,\ Ntotal}(x = 6 \text{ in.}) \qquad (5)$$

If any of the parameters N_1, m, and Q were found to be related, the relationships could be used to reduce the variability in $F_{a,\ Ntotal}(x)$. In the tests reported here, there was statistically significant correlation between Q and m in the corroded sample. There was weaker correlation between Q and m in the non-corroded sample.

Damage tolerance inspections of a fuselage skin splice are costly. Equations (1) to (5) and the associated Monte Carlo simulation could be used to help in selecting an inspection threshold and interval that will provide an acceptably low risk of fatigue failure at minimum cost. This analysis would require knowledge of the probability of crack detection (POD) characteristics of the chosen method of non-destructive inspection.

For illustrative purposes, the model has been applied in a simplified way using the mean value of the parameters N_1 and m and the correlation between m and Q to estimate the mean whole life to failure. The results of this analysis are summarised in Figure 16-12. The reduction in mean whole life due to corrosion was 32%. The model predicted 29%. In Corroded Sample B the reduction was 42%. The model

predicted 40%. As mentioned earlier, some of the corroded tests were terminated early. If the test lives had been adjusted to compensate, it is estimated that these test and model statistics would have been closer. The relative contributions of the hidden and detectable periods of crack growth are shown in each bar. The graph serves to confirm that there are no major inconsistencies between the model and the test data. It also highlights the longer period of detectable crack growth in corroded specimens. This was probably due to the reduced tendency for MSD in the corroded specimens.

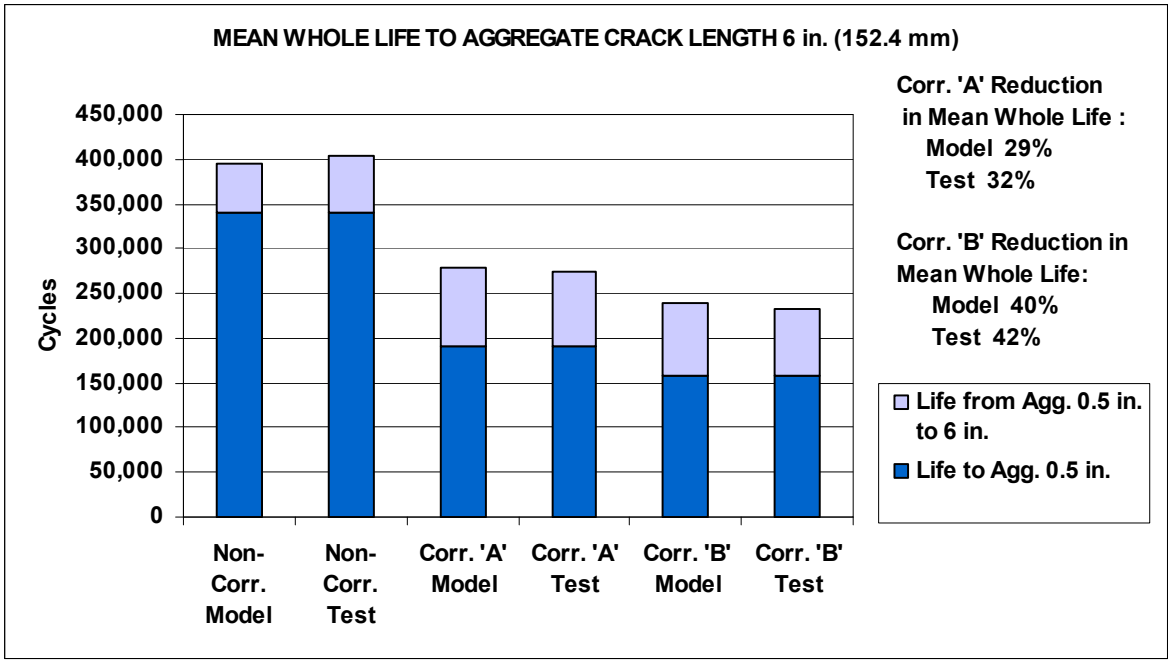

Figure 16-12: Graph of Mean Whole Life to an Aggregate Crack Length of 6 in. (152.4 mm), Showing the Relative Contributions of the Hidden and Detectable Periods of Crack Growth.

16.4 CONCLUSIONS

This section has described an experimental procedure that has been developed for evaluating the effect of prior corrosion on the fatigue characteristics of longitudinal fuselage skin splices in transport aircraft. The detailed design of the test specimen must be tailored to the aircraft splice to be studied.

It has been shown how the data from the experimental procedure can be used to construct a probabilistic model of fatigue life and crack growth in a splice where MSD is occurring. The model is applicable to non-corroded and corroded specimens.

The experimental procedure and the model have been demonstrated using a specimen design that is approximately representative of the types of single shear lap splices that are in use on several military and civil transport aircraft. Despite the complexity of the component and the variability of corrosion, statistically significant test results were obtained. These give confidence that the empirical modeling approach could have wide applicability.

The test data indicate that prior corrosion reduced the mean fatigue life to the detection of the first crack by 44%. The mean whole fatigue life was reduced by a lesser amount, 32%, because corrosion extended the period of detectable crack growth. This extension resulted mainly from a reduced tendency for MSD in corroded specimens.

The experimental procedure and model could be used to provide key input data for the durability and damage tolerance analysis of a fuselage skin splice. By taking corrosion fatigue interaction into account in this way, a more cost-effective design and maintenance policy might be achieved while maintaining or improving safety.

16.5 ACKNOWLEDGEMENTS

This work was a team effort involving many individuals at the NRC Institute for Aerospace Research, Carleton University, and Defence R&D Canada. In particular, Mr. D.V. Krizan and Mr. J.C. Cook of Carleton University and Mr. T.J. Benak of the NRC made a substantial contribution to the experimental work. Funding for the design, development, manufacture, and pre-corrosion of the test specimens, for the pilot test program (not described), and for part of the fatigue testing described in this paper was provided by the NRC and Defence R&D Canada. Part of the fatigue testing was supported by Lockheed Martin Aeronautics under the USAF Corrosion Fatigue Structural Demonstration (CFSD) Program (Contract RW26923, USAF prime contract F33165-97-C-3218).

16.6 REFERENCES

[1] Schütz, W., “Corrosion Fatigue the Forgotten Factor”, Proceedings of the 18th Symposium of the International Committee on Aeronautical Fatigue, Melbourne, Victoria, Australia, 3-5 May 1995.

[2] Kinzie, R., “Cost of Corrosion”, Proceedings of the 6th Joint FAA/DoD/NASA Conference on Aging Aircraft, San Francisco, CA, USA, 16-19 September 2002.

[3] Brooks, C.L. and Simpson, D.L., “Integrating Real Time Age Degradation Into the Structural Integrity Process”, Proc. Conf. Fatigue in the Presence of Corrosion, RTO-MP-18, NATO/RTO, March 1999.

[4] Eastaugh, G.F, Simpson, D.L., Straznicky, P.V. and Wakeman, R.B., “A Special Uniaxial Coupon Test Specimen for the Simulation of Multiple Site Fatigue Crack Growth and Link-Up in Fuselage Splices”, AGARD-CP-568, NATO/AGARD, pp. 2-1 – 2-19, December 1995.

[5] Eastaugh, G.F., Merati, A.A., Simpson, D.L., Straznicky, P.V., Scott, J.P., Wakeman, R.B. and Krizan, D.V., “An Experimental Study of Corrosion/Fatigue Interaction in the Development of Multiple Site Damage in Longitudinal Fuselage Skin Splices”, Proc. Conf. Fatigue in the Presence of Corrosion, RTO-MP-18, NATO/RTO, March 1999.

[6] Bellinger, N.C. and Komorowski, J.P., “Corrosion Pillowing Stresses in Fuselage Lap Joints”, AIAA Journal, Vol. 35, No. 2, pp. 317-320, February 1997.

[7] Little, R.E. and Jebe, E.H., “Manual on Statistical Planning and Analysis for Fatigue Experiments”, ASTM STP 588, American Society for Testing and Materials, Philadelphia, PA, USA, 1975.

[8] Manning, S.D. and Yang, J.N., “USAF Durability Design Handbook”, AFWAL-TR-88-3119, February 1989.

[9] Liao, M. and Yang, Q.X., “A Probabilistic Model for Fatigue Crack Growth”, Engineering Fracture Mechanics, Vol. 43, No. 4, pp. 651-655, 1992.